19. He S, McPhaul C, Li JZ, Garuti R, Kinch L, et al. (2010) A Sequence Variation (I148M) in PNPLA3 Associated with Nonalcoholic Fatty Liver Disease Disrupts Triglyceride Hydrolysis. J Biol Chem 285: 6706–6715. doi:10.1074/jbc.M109.064501.
20. Ueno T, Inuzuka S, Torimura T, Tamaki S, Koh H, et al. (1993) Serum hyaluronate reflects hepatic sinusoidal capillarization. Gastroenterology 105: 475–481.
21. Brunt EM, Janney CG, Di Bisceglie AM, Neuschwander-Tetri BA, Bacon BR (1999) Nonalcoholic steatohepatitis: a proposal for grading and staging the histological lesions. Am J Gastroenterol 94: 2467–2474. doi:10.1111/j.1572–0241.1999.01377.x.
22. Suzuki T, Matsuo K, Sawaki A, Mizuno N, Hiraki A, et al. (2008) Alcohol Drinking and One-Carbon Metabolism-Related Gene Polymorphisms on Pancreatic Cancer Risk. Cancer Epidemiology Biomarkers & Prevention 17: 2742–2747. doi:10.1158/1055–9965.EPI-08–0470.
23. Purcell S, Neale B, Todd-Brown K, Thomas L, Ferreira MAR, et al. (2007) PLINK: A Tool Set for Whole-Genome Association and Population-Based Linkage Analyses. Am J Hum Genet 81: 559–575.
24. Yamada R, Okada Y (2009) An optimal dose-effect mode trend test for SNP genotype tables. Genet Epidemiol 33: 114–127. doi:10.1002/gepi.20362.
25. Devlin B, Roeder K (1999) Genomic control for association studies. Biometrics 55: 997–1004.
26. Barrett JC, Fry B, Maller J, Daly MJ (2005) Haploview: analysis and visualization of LD and haplotype maps. Bioinformatics 21: 263–265. doi:10.1093/bioinformatics/bth457.

Original Article

Defining Patients at Extremely High Risk for Coronary Artery Disease in Heterozygous Familial Hypercholesterolemia

Takako Sugisawa[1], Tomonori Okamura[2], Hisashi Makino[1], Makoto Watanabe[3], Ichiro Kishimoto[1], Yoshihiro Miyamoto[3], Noriyuki Iwamoto[1], Akira Yamamoto[4], Shinji Yokoyama[5] and Mariko Harada-Shiba[1,6]

[1]Division of Endocrinology and Metabolism, National Cerebral and Cardiovascular Center, Japan
[2]Department of Public Health and Preventive Medicine, Keio University, Japan
[3]Department of Preventive Cardiology, National Cerebral and Cardiovascular Center, Japan
[4]Health Care Facilities for the Aged, Minoh Life Plaza, Japan
[5]Food and Nutritional Sciences, College of Bioscience and Biotechnology, Chubu University, Japan
[6]Department of Molecular Innovation in Lipidology, National Cerebral and Cardiovascular Center Research Institute, Osaka, Japan

Aim: **Heterozygous patients with familial hypercholesterolemia (FH) are known to be associated with a high risk of coronary artery disease (CAD), which is a major determinant of their clinical outcome. The prognosis of heterozygous FH patients substantially varies, being dependent on the level of their CAD risk, and their therapeutic regimen should be individualized. We assessed critical levels of LDL-cholesterol (LDL-C) and Achilles tendon thickness (ATT) to identify heterozygous FH patients at "very high" risk for CAD.**

Methods: **One hundred and nine heterozygous FH patients who had no history of CAD and had had their plasma lipid profile and ATT assessed before treatment were followed up until their first CAD event or 31 December 2010. Multivariable logistic regression models were used to analyze the correlation of LDL-C and/or ATT levels with the risk of developing CAD.**

Results: **During the follow-up period, 21 of the 109 patients had a CAD event, diagnosed by coronary angiogram. Individuals in the highest tertile of LDL-C had a CAD risk 8.29-fold higher than those in the lowest tertile. Individuals in the highest tertile of the ATT group had a 7.82-fold higher CAD risk than those in the lowest tertile. Those who had either LDL-C ≥ 260 mg/dL or ATT ≥ 14.5 had a 23.94-fold higher CAD risk than those with LDL-C < 260 mg/dL and ATT < 14.5 mm.**

Conclusions: **In heterozygous FH patients, LDL-C 260 mg/dL or higher and/or ATT 14.5 mm or thicker are useful markers for extracting patients at "very high" risk for CAD.**

J Atheroscler Thromb, 2012; 19:369-375.

Key words; Familial hypercholesterolemia, LDL cholesterol, Coronary artery disease, Coronary risk, Achilles tendon thickness

Introduction

Familial hypercholesterolemia (FH) is an autosomal dominant disorder characterized by hypercholesterolemia, skin and tendon xanthomas and a high risk of coronary artery disease (CAD) due to premature atherosclerosis[1]. FH has the highest prevalence in genetic metabolic diseases, showing one per 300 to 500 heterozygous patients in the general population[1,2]. High low-density lipoprotein cholesterol (LDL-C) is the first symptom, appearing in heterozygous FH even from birth, and xanthomas in the Achilles tendon usually appear during or after the late 10s and are found in half of all patients by the age of 30[1]. Coronary artery disease (CAD), which determines the prognosis of FH patients, appears during or after the third decade of life in men and the fifth decade in women[3-5].

Address for correspondence: Mariko Harada-Shiba, Department of Molecular Innovation in Lipidology, National Cerebral and Cardiovascular Center Research Institute, 5-7-1 Fujishiro-dai, Suita, Osaka, 565-8565, Japan
E-mail: shiba.mariko.ri@mail.ncvc.go.jp
Received: August 23, 2011
Accepted for publication: October 14, 2011

CAD mortality in heterozygous FH is several times higher than that in the general population[1, 6-8]; therefore, it is very important to prevent CAD in heterozygous FH patients. The prognosis of heterozygous patients of FH varies substantially, such that some develop CAD at their 20s while others may not develop CAD until their seventh decade; therefore, the therapeutic regimen should be individualized according to the patients' risk of CAD.

Various risk factors for CAD have been identified in heterozygous patients with FH, such as age, sex, LDL-C, triglyceride (TG), HDL-C, Achilles tendon thickness (ATT), smoking, a family history of CAD, hypertension, diabetes mellitus, Lp(a), homocysteine and so on[3, 9-12]. Among these parameters, LDL-C and ATT are simple, specific and non-invasive to measure, and can easily be used by primary care physicians to evaluate the CAD risk. We therefore estimated the CAD risks in accordance with LDL-C and ATT in heterozygous FH patients in order to identify those at extremely high risk.

Methods

Subjects

Of the patients referred to the lipid clinic at the National Cerebral and Cardiovascular Center (NCVC) from 1977 to 2007, 329 consecutive patients diagnosed as FH heterozygotes using previously described criteria[6] were subjected to this study. After diagnosis, the FH patients had medical checks according to the standard procedure for treating heterozygous FH in NCVC. The patients were subjected to a treadmill test for CAD screening just after their first visit to our clinic. Those who had a positive result on the treadmill test were subjected to a coronary angiogram (CAG), and diagnosed with CAD with 75% or more stenosis. Those who had a negative result on the treadmill or no significant stenosis by CAG were included in this study. Among the 329 FH patients, 229 were excluded: 53 had a past history of CAD, 160 had not had LDL-C measured before treatment, 76 had not had ATT thickness measured and 3 had TG more than 4.5 mmol/L, so 109 were followed up until their first CAD event or 31 December 2010. After the first visit to our clinic, dietary and drug treatment, including statins, was immediately started and continued.

During the course, those who had chest pain or a positive result on the treadmill test performed biennially were subjected to CAG, and diagnosed with CAD with 75% or more stenosis. Medical records of the patients were examined according to the analysis protocol approved by our institutional ethics committee (ID#M20-25-2).

Clinical and Laboratory Characteristics

Serum lipid and lipoprotein levels were measured at the time of initial diagnosis, before any lipid-lowering treatment. TC, TG and HDL-C levels were measured enzymatically with a commercial kit (Daiichi Pure Chemicals Co., Tokyo, Japan) using an automated analyzer (Hitachi model 704; Hitachi, Tokyo, Japan) in the clinical laboratory of the National Cerebral and Cardiovascular Center (NCVC). LDL-C was calculated by the Friedewald formula. ATT was measured by X-ray according to the method previously described[13]. Body mass index (BMI) was calculated as weight in kilograms divided by height in meters squared (kg/m^2). Hypertension was defined as the use of antihypertensive drugs or blood pressure $\geq$140 mmHg systolic or $\geq$90 mmHg diastolic or both at the first clinic visit (the criteria for hypertension of the Japanese Society of Hypertension Guidelines)[14]. Diabetes mellitus was defined according to the 2002 Guideline for the Treatment of Diabetes Mellitus of the Japanese Diabetes Society[15]. A family history of CAD was defined as positive by having within 2nd degree family members with CAD on the standardized questionnaire. Smoking was defined as positive by having a smoking habit at the first visit to NCVC on the patient report.

Statistical Analyses

Continuous variables are presented as the means $\pm$ SDs. Categorical data are presented as numbers and percentages. Unpaired Student's *t*-test and one-way analysis of variance (ANOVA) were used to assess differences between groups in continuous variables. Differences in categorical variables were assessed by the χ^2 test.

Multivariable logistic regression analysis after adjusting for age, sex, hypertension, diabetes mellitus, smoking, family history of CAD, and low HDL-C ($<$40 mg/dL) were used to analyze correlations of LDL-C levels or ATT levels and the development of CAD. LDL-C levels were categorized into tertiles: (1) LDL-C $<$206 mg/dL, (2) LDL $\geq$206 and $<$260 mg/dL, (3) LDL-C $\geq$260 mg/dL. ATT levels were also categorized into tertiles: (1) ATT $<$9.0 mm, (2) ATT $\geq$9.0 mm and $<$14.5 mm, (3) ATT $\geq$14.5 mm. All the confidence intervals were estimated at the 95% level and significance was set at $p<0.05$. All data were analyzed with the SPSS version 16.0 (SPSS Inc., Chicago, IL, USA) statistical software package.

Table 1. Clinical characteristics of 109 patients with heterozygous FH classified with or without CAD

	Total $n=109$	CAD(−) $n=88$	CAD(+) $n=21$	p value
Age (years)	41.9 ± 16.2	39.7 ± 16.7	50.9 ± 10.5	<0.01
Sex (male), n (%)	43 (39.4%)	30 (34.1%)	12 (57.1%)	0.052
Achilles tendon thickness (mm)	12.6 ± 5.4	11.5 ± 4.5	17.4 ± 6.3	<0.0001
Skin xanthomas, n (%)	25 (22.9%)	16 (18.2%)	9 (42.9%)	0.052
Arcus cornea, n (%)	45 (41.3%)	27 (30.7%)	16 (76.2%)	0.001
Total cholesterol (mg/dL)	321 ± 68	309 ± 56	368 ± 92	<0.001
Triglyceride (mg/dL)	139 ± 82	134 ± 85	156 ± 65	0.272
HDL-C (mg/dL)	51 ± 15	51 ± 15	50 ± 15	0.747
LDL-C (mg/dL)	242 ± 70	232 ± 59	287 ± 92	0.001
Smoking (past or current), n (%)	42 (38.5%)	28 (31.8%)	14 (66.6%)	0.003
Hypertension, n (%)	19 (17.4%)	10 (11.4%)	9 (42.9%)	0.003
Diabetes mellitus, n (%)	9 (8.2%)	5 (5.7%)	4 (19.0%)	0.186
Family history of CAD, n (%)	47 (43.1%)	37 (42.0%)	10 (47.6%)	0.411

Table 2. Clinical characteristics at first visit in heterozygous patients of FH classified by LDL-C Levels (Mean ± SD)

LDL-C (mg/dL) categories	LDL-C < 206 $n=36$	206 ≦ LDL-C < 260 $n=36$	LDL-C ≥ 260 $n=37$	p value
Age (years)	43.7 ± 15.6	42.0 ± 17.5	40.0 ± 15.8	0.645
Sex (male), n (%)	14 (38.9%)	13 (36.1%)	15 (40.5%)	0.928
Body mass index (kg/m^2)	22.2 ± 3.3	22.5 ± 3.2	22.8 ± 6.8	0.880
Total cholesterol (mg/dL)	258 ± 28	308 ± 20	394 ± 55	<0.001
Triglyceride (mg/dL)	149 ± 102	134 ± 67	134 ± 74	0.672
HDL-C (mg/dL)	54 ± 16	51 ± 15	47 ± 14	0.100
Smoking (past or current), n (%)	15 (41.7%)	10 (27.8%)	15 (40.5%)	0.385
Hypertension, n (%)	5 (13.9%)	6 (16.7%)	3 (8.1%)	0.660
Diabetes mellitus, n (%)	2 (5.6%)	3 (8.3%)	2 (5.4%)	0.831
Family history of CAD, n (%)	17 (47.2%)	14 (38.9%)	16 (43.2%)	0.775
Achilles tendon thickness (mm)	10.7 ± 4.2	12.5 ± 5.5	14.6 ± 5.8	0.282
CAD, n (%)	5 (13.9%)	3 (8.3%)	13 (35.1%)	0.02

Results

Characteristics of the Patients Subjected to Analysis of the Correlations of LDL-C and CAD

Among 109 patients, 21 (19.3%) developed CAD during the subsequent period. There was a significantly higher prevalence of hypertension, skin xanthomas, arcus cornea and smoking in the CAD (+) group. Mean age, ATT, TC and LDL-C were significantly higher in the CAD (+) group than in the CAD (−) group (**Table 1**).

LDL-C Levels and Development of CAD

The clinical characteristics of patients categorized into tertiles according to their LDL-C levels are shown in **Table 2**. They clearly show that parameters other than TC levels were not significantly different in each tertile. Higher LDL-C was associated with higher TC and the incidence of CAD.

To examine the influence of conventional coronary risk factors, logistic regression analyses for CAD were performed. The multivariable adjusted odds ratios (ORs) for CAD are shown in **Table 3**. Individuals in the highest tertile (LDL-C ≥ 260 mg/dL) had a 8.29-fold increased risk of CAD incidence compared with those in the lowest tertile (LDL-C < 206 mg/dL) (adjusted odds ratio (OR) 8.29, 95 % CI 1.33-51.47, $p=0.023$). No significant increase in the odds of future CAD in the second tertile (206 ≦ LDL-C < 260 mg/dL) (adjusted OR 0.42, 95%CI 0.05-3.26, $p=0.409$).

Table 3. Multivariate-adjusted odds ratio for CAD by logistic regression analyses according to LDL-C

LCL-C categories	n	Odds Ratio	95% CI	*p* value
LDL-C < 206 mg/dL	36	1.0 (referent)	–	–
206 ≦ LDL-C < 260 mg/dL	36	0.42	0.05-3.26	0.409
LDL-C ≥ 260 mg/dL	37	8.29	1.33-51.47	0.023

Multivariable logistic regression models for CAD are adjusted for age, sex, hypertension, diabetes mellitus, smoking, family history of CAD, and low HDL-C (< 40 mg/dL).

Table 4. Clinical characteristics at first visit in heterozygous patients of FH classified by ATT levels (mean ± SD)

ATT (mm) categories	ATT < 9 *n*=36	9 ≦ ATT < 14.5 *n*=37	ATT ≥ 14.5 *n*=36	*p* value
Age (years)	39.7 ± 18.3	39.4 ± 16.4	45.2 ± 13.5	0.177
Sex (male), n (%)	11 (30.6%)	13 (35.1%)	18 (50.0%)	0.207
BMI (kg/m^2)	22.3 ± 2.8	21.7 ± 2.8	23.1 ± 2.7	0.883
Total cholesterol (mg/dL)	293 ± 42	319 ± 66	350 ± 79	0.002
Triglycerides (mg/dL)	140 ± 106	134 ± 69	142 ± 67	0.505
HDL-C (mg/dL)	57 ± 14	47 ± 14	48 ± 15	0.916
LDL-C (mg/dL)	208 ± 44	245 ± 67	274 ± 78	0.003
Smoking habit, n (%)	9 (25.0%)	13 (35.1%)	14 (38.9%)	0.001
Hypertension, n (%)	4 (11.1%)	2 (5.4%)	8 (22.2%)	0.094
Diabetes mellitus, n (%)	1 (2.8%)	1 (2.7%)	5 (13.9%)	0.125
Family history of CAD, n (%)	16 (44.4%)	17 (46.0%)	14 (38.9%)	0.815
CAD, n (%)	2 (5.6%)	4 (10.8%)	15 (41.7%)	< 0.001

ATT Levels and Development of CAD

The clinical characteristics of patients categorized into tertiles according to their ATT levels are shown in **Table 4**. Higher ATT levels were associated with higher TC and LDL-C levels, smoking and the incidence of CAD.

The multivariable adjusted OR for CAD is shown in **Table 5**. Individuals in the highest tertile group of ATT ≥ 14.5 mm had a 7.82-fold increased risk of CAD compared with those in the ATT < 9.0 mm group (95%CI 1.28-47.7, p=0.001). No significant increase in the odds of future CAD in the group with 9 ≦ ATT < 14.5 mm (adjusted OR 1.42, 95%CI 0.18-11.14, p=0.740).

LDL-C and/or ATT Levels and Development of CAD

To estimate the future risk for CAD using the combination of LDL-C and ATT thickness, the patients were divided into 3 groups, (1) LDL-C < 260 mg/dL and ATT < 14.5 mm, (2) LDL-C < 260 and ATT ≥ 14.5, or LDL-C ≥ 260 and ATT < 14.5, (3) LDL-C ≥ 260 and ATT ≥ 14.5. OR for CAD was calculated for these groups and shown in **Table 6**. Those who had both LDL-C ≥ 260 and ATT ≥ 14.5 had a 20.62-fold increased risk of CAD compared with those with LDL-C < 260 and ATT < 14.5 (95%CI 2.91-145.89). Those with either LDL-C ≥ 260 or ATT ≥ 14.5 had a 23.62-fold increased risk of CAD compared with those with LDL-C < 260 and ATT < 14.5 (95%CI 3.11-184.16).

Discussion

As the prognosis of heterozygous FH patients varies substantially, the therapeutic regimen should be determined according to the CAD risk of individual patients. High levels of LDL-C and ATT are clinical signs already found at a young age and can be measured easily and non-invasively by family physicians in primary care, so they can be good markers for estimating the future CAD risk of FH. In the present study, we demonstrated the critical levels of LDL-C and ATT for estimation of the CAD risk in Japanese heterozygous patients with FH.

Several studies on the Japanese population have indicated that the serum cholesterol level is correlated significantly with the risk of CAD[16, 17]. The increased CAD incidence seems exponential with the serum cholesterol level in the general population, and it can be

Table 5. Multivariate-adjusted odds ratio for CAD by logistic regression analyses according to ATT levels

ATT (mm) categories	n	Odds Ratio	95% CI	*p* value
ATT < 9 mm	36	1.0 (referent)	–	–
9 ≦ ATT < 14.5 mm	37	1.42	0.18-11.14	0.740
ATT ≥ 14.5 mm	36	7.82	1.28-47.7	0.001

Multivariable logistic regression models for CAD are adjusted for age, sex, hypertension, diabetes mellitus, smoking, family history of CAD and low HDL-C (< 40 mg/dL).

Table 6. Multivariate-adjusted odds ratio for CAD by logistic regression analyses according to both ATT and LDL-C levels

LDL-C and ATT categories	n	Odds Ratio	95% CI	*p* value
LDL-C < 260, ATT < 14.5 mm	54	1.0 (referent)	–	–
LDL-C < 260, ATT ≥ 14.5 mm or LDL-C ≥ 260, ATT < 14.5 mm	37	23.94	3.11-184.16	0.002
LDL-C ≥ 260, ATT ≥ 14.5 mm	18	20.62	2.91-145.89	0.002

Multivariable logistic regression models for CAD are adjusted for age, sex, hypertension, diabetes mellitus, smoking, family history of CAD and low HDL-C (< 40 mg/dL).

considered low until it hits a certain "threshold". The findings of the relationship with LDL-C levels and the onset of CAD in FH patients seem to show a "right shift" of this profile as LDL-C 2-fold higher and CAD incidence more than 10-fold. Previous studies have reported that higher LDL-C is related with the higher risk factors for the development of CAD even in heterozygous FH patients[18, 19], whereas other factors, such as age, gender, hypertension, smoking, or other lipid abnormalities, such as low HDL-C and high TG reportedly contribute to the increased risk[3, 12, 18-22]. Bujo *et al.* reported that male gender, age over 50, smoking, hypertension, diabetes mellitus, TG >150 mg/dL and HDL-C <40 mg/dL were risk factors for CAD in FH by multicenter, cross-sectional analysis[3].

As we reported in a previous paper, drug treatment including statins may influence the outcome of CAD[5]. The name and dose of drugs prescribed to the patients during the course are listed in **Table 7**. Because all FH patients had had intensive drug therapy to prevent the development of atherosclerosis, no comparison could be made with those without drug therapy. It was also impossible to analyze the difference in drugs statistically because there were so many patterns of prescription and most patients changed the type and dose of drugs several times during the course.

LDL-C levels under drug treatment may also affect the outcome. The mean LDL-C under drug treatment did not increase the odds ratio for CAD (odds ratio: 0.983, 95%CI: 0.97-1.00); however the relationship between mean LDL-C in the pre-treatment period and CAD risk remained due to pre-exposure to high LDL-C before treatment, although the absolute risk of CAD might be decreased at any LDL-C level by intensive drug treatment during the course.

Table 7. Lipid-lowering drugs in heterozygous FH patients during the course

	Dose/day
cholestyramine	4-12 g
colestimide	0.5-3 g
probucol	250-1,000 mg
pravastatin	10-30 mg
simvastatin	5-20 mg
fluvastatin	20-60 mg
atorvastatin	5-40 mg
pitavastatin	1-4 mg
rosuvastatin	2.5-20 mg
fenofibrate	100-200 mg
bezafibrate	100-400 mg
ezetimibe	5-10 mg

Civerira *et al.* reported that heterozygous FH with tendon xanthomas has a 3.1-fold increased risk of premature CAD compared with those without it[23]. The Achilles tendon was reported to be thicker in FH patients with CAD than in those without CAD in both sexes[12]. Persistent high LDL-C causes cholesterol depositions in the tendons and results in tendon xanthomas[1]. Achilles tendon xanthomas have been used

as one of the criteria for clinical diagnosis of FH because of their high sensitivity and specificity[1, 24]. A strongly positive correlation was observed between ATT and cholesterol-year scores in FH patients[25, 26], suggesting that ATT reflects both the severity and duration of hypercholesterolemia. ATT is an important factor that can be measured quantitatively as the deposition of cholesterol in the tissue. The present study showed that ATT is a good marker for evaluating the risk for CAD, indicating that there is a strong correlation between the deposition of cholesterol in extravascular tissue and the stenosis of coronary arteries. ATT should be used not only as a diagnostic parameter for FH but also, and more importantly, as a prognostic factor that indicates the need for a more aggressive approach for patients at high risk.

In conclusion, LDL-C ≥260 mg/dL and ATT ≧14.5 mm or thicker are useful criteria for identifying patients at "very high" risk of CAD in Japanese heterozygous FH. Patients with either of these risk factors require more intensive cholesterol-lowering therapy and a more careful medical check-up for CAD.

Acknowledgments

This work was supported by Grants-in-Aid for Scientific Research from the Japanese Ministry of Health, Labor and Welfare (H23-seisakutansaku-ippan-004 and H20-nanji-ippan-011) and the Cardiovascular Research Foundation (Suita, Japan).

References

1) Goldstein JL, Hobbs H, Brown MS: Familial hypercholesterolemia. Edited by Scriver CR BA, Sly WS, Valle D, pp2863-2913, McGraw-Hill, New York, 2001
2) Mabuchi H, Nohara A, Noguchi T, Kobayashi J, Kawashiri MA, Tada H, Nakanishi C, Mori M, Yamagishi M, Inazu A, Koizumi J: Molecular genetic epidemiology of homozygous familial hypercholesterolemia in the Hokuriku district of Japan. Atherosclerosis, 2011; 214: 404-407
3) Bujo H, Takahashi K, Saito Y, Maruyama T, Yamashita S, Matsuzawa Y, Ishibashi S, Shionoiri F, Yamada N, Kita T: Clinical features of familial hypercholesterolemia in Japan in a database from 1996-1998 by the research committee of the ministry of health, labour and welfare of Japan. J Atheroscler Thromb, 2004; 11: 146-151
4) Mabuchi H, Koizumi J, Shimizu M, Takeda R: Development of coronary heart disease in familial hypercholesterolemia. Circulation, 1989; 79: 225-232
5) Harada-Shiba M, Sugisawa T, Makino H, Abe M, Tsushima M, Yoshimasa Y, Yamashita T, Miyamoto Y, Yamamoto A, Tomoike H, Yokoyama S: Impact of statin treatment on the clinical fate of heterozygous familial hypercholesterolemia. J Atheroscler Thromb, 17: 667-674
6) Mabuchi H, Miyamoto S, Ueda K, Oota M, Takegoshi T, Wakasugi T, Takeda R: Causes of death in patients with familial hypercholesterolemia. Atherosclerosis, 1986; 61: 1-6
7) Jensen J, Blankenhorn DH, Kornerup V: Coronary disease in familial hypercholesterolemia. Circulation, 1967; 36: 77-82
8) Stone NJ, Levy RI, Fredrickson DS, Verter J: Coronary artery disease in 116 kindred with familial type II hyperlipoproteinemia. Circulation, 1974; 49: 476-488
9) Yagi K, Hifumi S, Nohara A, Higashikata T, Inazu A, Mizuno KO, Namura M, Ueda K, Kobayashi J, Shimizu M, Mabuchi H: Difference in the risk factors for coronary, renal and other peripheral arteriosclerosis in heterozygous familial hypercholesterolemia. Circ J, 2004; 68: 623-627
10) Pisciotta L, Cortese C, Gnasso A, Liberatoscioli L, Pastore A, Mannucci L, Irace C, Federici G, Bertolini S: Serum homocysteine, methylenetetrahydrofolate reductase gene polymorphism and cardiovascular disease in heterozygous familial hypercholesterolemia. Atherosclerosis, 2005; 179: 333-338
11) Real JT, Martinez-Hervas S, Garcia-Garcia AB, Chaves FJ, Civera M, Ascaso JF, Carmena R: Association of C677T polymorphism in MTHFR gene, high homocysteine and low HDL cholesterol plasma values in heterozygous familial hypercholesterolemia. J Atheroscler Thromb, 2009; 16: 815-820
12) Hirobe K, Matsuzawa Y, Ishikawa K, Tarui S, Yamamoto A, Nambu S, Fujimoto K: Coronary artery disease in heterozygous familial hypercholesterolemia. Atherosclerosis, 1982; 44: 201-210
13) Mabuchi H, Ito S, Haba T, Ueda K, Ueda R: Discrimination of familial hypercholesterolemia and secondary hypercholesterolemia by Achilles' tendon thickness. Atherosclerosis, 1977; 28: 61-68
14) Ikeda N, Hasegawa T, Hasegawa T, Saito I, Saruta T: Awareness of the Japanese Society of Hypertension Guidelines for the Management of Hypertension (JSH 2000) and compliance to its recommendations: surveys in 2000 and 2004. J Hum Hypertens, 2006; 20: 263-266
15) Matsushima M: [Japan Diabetes Society clinical practice guideline]. Nippon Rinsho, 2002; 60 Suppl 9: 161-166
16) Nakamura Y, Yamamoto T, Okamura T, Kadowaki T, Hayakawa T, Kita Y, Saitoh S, Okayama A, Ueshima H: Combined cardiovascular risk factors and outcome: NIPPON DATA80, 1980-1994. Circ J, 2006; 70: 960-964
17) Okamura T, Kokubo Y, Watanabe M, Higashiyama A, Miyamoto Y, Yoshimasa Y, Okayama A: Low-density lipoprotein cholesterol and non-high-density lipoprotein cholesterol and the incidence of cardiovascular disease in an urban Japanese cohort study: The Suita study. Atherosclerosis, 2009; 203: 587-592
18) Hill JS, Hayden MR, Frohlich J, Pritchard PH: Genetic and environmental factors affecting the incidence of coronary artery disease in heterozygous familial hypercholesterolemia. Arterioscler Thromb, 1991; 11: 290-297
19) Ferrieres J, Lambert J, Lussier-Cacan S, Davignon J: Cor-

onary artery disease in heterozygous familial hypercholesterolemia patients with the same LDL receptor gene mutation. Circulation, 1995; 92: 290-295
20) Seed M, Hoppichler F, Reaveley D, McCarthy S, Thompson GR, Boerwinkle E, Utermann G: Relation of serum lipoprotein(a) concentration and apolipoprotein(a) phenotype to coronary heart disease in patients with familial hypercholesterolemia. N Engl J Med, 1990; 322: 1494-1499
21) Wiklund O, Angelin B, Olofsson SO, Eriksson M, Fager G, Berglund L, Bondjers G: Apolipoprotein(a) and ischaemic heart disease in familial hypercholesterolaemia. Lancet, 1990; 335: 1360-1363
22) Yanagi K, Yamashita S, Kihara S, Nakamura T, Nozaki S, Nagai Y, Funahashi T, Kameda-Takemura K, Ueyama Y, Jiao S, Kubo M, Tokunaga K, Matsuzawa Y: Characteristics of coronary artery disease and lipoprotein abnormalities in patients with heterozygous familial hypercholesterolemia associated with diabetes mellitus or impaired glucose tolerance. Atherosclerosis, 1997; 132: 43-51
23) Civeira F, Castillo S, Alonso R, Merino-Ibarra E, Cenarro A, Artied M, Martin-Fuentes P, Ros E, Pocovi M, Mata P: Tendon xanthomas in familial hypercholesterolemia are associated with cardiovascular risk independently of the low-density lipoprotein receptor gene mutation. Arterioscler Thromb Vasc Biol, 2005; 25: 1960-1965
24) Sullivan D: Guidelines for the diagnosis and management of familial hypercholesterolaemia. Heart Lung Circ, 2007; 16: 25-27
25) Schmidt HH, Hill S, Makariou EV, Feuerstein IM, Dugi KA, Hoeg JM: Relation of cholesterol-year score to severity of calcific atherosclerosis and tissue deposition in homozygous familial hypercholesterolemia. Am J Cardiol, 1996; 77: 575-580
26) Lehtonen A, Makela P, Viikari J, Virtama P: Achilles tendon thickness in hypercholesterolaemia. Ann Clin Res, 1981; 13: 39-44

Diabetologia (2012) 55:1689–1698
DOI 10.1007/s00125-012-2508-2

ARTICLE

Induced pluripotent stem cells generated from diabetic patients with mitochondrial DNA A3243G mutation

J. Fujikura · K. Nakao · M. Sone · M. Noguchi · E. Mori · M. Naito · D. Taura · M. Harada-Shiba · I. Kishimoto · A. Watanabe · I. Asaka · K. Hosoda · K. Nakao

Received: 4 December 2011 / Accepted: 30 January 2012 / Published online: 7 March 2012

Abstract
Aims/hypothesis The aim of this study was to generate induced pluripotent stem (iPS) cells from patients with mitochondrial DNA (mtDNA) mutation.
Methods Skin biopsies were obtained from two diabetic patients with mtDNA A3243G mutation. The fibroblasts thus obtained were infected with retroviruses encoding *OCT4* (also known as *POU5F1*), *SOX2*, *c-MYC* (also known as *MYC*) and *KLF4*. The stem cell characteristics were investigated and the mtDNA mutation frequencies evaluated by Invader assay.
Results From the two diabetic patients we isolated four and ten putative mitochondrial disease-specific iPS (Mt-iPS) clones, respectively. Mt-iPS cells were cytogenetically normal and positive for alkaline phosphatase activity, with the pluripotent stem cell markers being detectable by immunocytochemistry. The cytosine guanine dinucleotide islands in the promoter regions of *OCT4* and *NANOG* were highly unmethylated, indicating epigenetic reprogramming to pluripotency. Mt-iPS clones were able to differentiate into derivatives of all three germ layers in vitro and in vivo. The Mt-iPS cells exhibited a bimodal degree of mutation heteroplasmy. The mutation frequencies decreased to an undetectable level in six of 14 clones, while the others showed several-fold increases in mutation frequencies (51–87%) compared with those in the original fibroblasts (18–24%). During serial cell culture passage and after differentiation, no recurrence of the mutation or no significant changes in the levels of heteroplasmy were seen.
Conclusions/interpretation iPS cells were successfully generated from patients with the mtDNA A3243G mutation. Mutation-rich, stable Mt-iPS cells may be a suitable source of cells for human mitochondrial disease modelling in vitro. Mutation-free iPS cells could provide an unlimited, disease-free supply of cells for autologous transplantation therapy.

Keywords Gene therapy · Monogenic forms of diabetes · Stem cells

Abbreviations

EB	Embryoid body
ES	Embryonic stem
FOXA2	Forkhead box A2
iPS	Induced pluripotent stem
MELAS	Mitochondrial encephalopathy lactic acidosis and stroke-like episodes

Junji Fujikura and Kazuhiro Nakao contributed equally to this study.

Electronic supplementary material The online version of this article (doi:10.1007/s00125-012-2508-2) contains peer-reviewed but unedited supplementary material, which is available to authorised users.

J. Fujikura (✉) · K. Nakao · M. Sone · M. Noguchi · E. Mori · M. Naito · D. Taura · K. Nakao (✉)
Department of Medicine and Clinical Science,
Kyoto University Graduate School of Medicine,
54 Shogoin Kawahara-cho, Sakyo-ku,
Kyoto 606-8507, Japan
e-mail: j-fuji@sannet.ne.jp
e-mail: nakao@kuhp.kyoto-u.ac.jp

M. Harada-Shiba · I. Kishimoto
Department of Endocrinology and Metabolism,
National Cerebral and Cardiovascular Center,
Osaka, Japan

A. Watanabe · I. Asaka
Center for iPS Cell Research and Application (CiRA),
Institute for Integrated Cell-Material Sciences,
Kyoto, Japan

K. Hosoda
Department of Human Health Science,
Kyoto University Graduate School of Medicine,
Kyoto, Japan

MERRF	Myoclonic epilepsy and ragged-red fibres
Mt1	Mt-iPS patient 1
Mt2	Mt-iPS patient 2
mtDNA	Mitochondrial DNA
Mt-iPS	Mitochondrial disease-specific iPS
NANOG	Nanog homeobox
SCID	Severe combined immunodeficient
α-SMA	α-Smooth muscle actin
SOX	SRY (sex determining region Y)-box
SSEA	Stage-specific embryonic antigen
TRA	Tumour rejection antigen

Introduction

Mitochondrial DNA (mtDNA) is present inside mitochondria and codes for components essential for cellular energy production [1]. mtDNA mutations cause degenerative human diseases. The tRNA (Leu) A3243G mutation is one of the most frequently observed mutations of mtDNA and is associated with a wide range of clinical phenotypes, including diabetes mellitus, hearing loss, cardiomyopathy, and mitochondrial encephalopathy, lactic acidosis and stroke-like episodes (MELAS) [2].

The mode of inheritance of mitochondrial diseases is maternal, but the penetrance of the disease is variable [3]. It is not possible to predict the phenotypes of children on the basis of the mother's genotypes and phenotypes, because the segregation of mtDNA tends to follow a pattern of random genetic drift [3]. This is the case for somatic cells and germ cells: it is not possible to predict to which cell types mutant mtDNA will dominantly migrate during development. To date, there is no specific therapy or cure for mitochondrial diseases, only supportive treatment. Efforts to understand the underlying genetics and pathophysiology of mitochondrial diseases have been hampered by the lack of a disease model.

Recently, human induced pluripotent stem (iPS) cells were successfully induced from adult skin fibroblasts [4]. iPS cells are biologically indistinguishable from embryonic stem (ES) cells. Human iPS cells, like ES cells, can differentiate into a variety of cell types and may therefore be another cell source for regenerative medicine. We have previously reported on angiogenic and adipogenic differentiation of human iPS and ES cells [5, 6]. More recently, disease-specific iPS cells have been generated from fibroblasts obtained from patients with various diseases [7–14], although not with mitochondrial diseases. The purpose of the present study was to derive iPS cells from patients with mitochondrial diseases and to evaluate the mtDNA of these cells.

Methods

Generation of mitochondrial disease-specific iPS cells Skin biopsies were undertaken after informed consent under protocols approved by the Ethics Committee of Kyoto University. Skin samples (4 mm) were minced with scalpels into smaller pieces and tissue fragments were placed into a tissue culture dish under a sterile coverslip. Medium (DMEM supplemented with 10% FBS (wt/vol.) and penicillin/streptomycin; Invitrogen, Carlsbad, CA, USA) was added to completely immerse the coverslip, and dishes were incubated at 37°C in a humidified incubator (5% CO_2). Fibroblasts grew out of the tissue fragments and when sufficiently numerous, cells were trypsinised and expanded. Cell cloning by limiting dilution in 96-well microtitre plates was employed at passage five.

The generation of iPS cells was performed according to the protocol of Ohnuki et al. [15]. In brief, the mouse ecotropic retrovirus receptor *Slc7a1* gene (Addgene, www.addgene.org/) was introduced to patient-derived fibroblasts at around passage number four by infection with lentivirus for 24 h. Retrovirus production was carried out for 24 h in Plat-E packaging cells via transfection with pMXs-hOCT4, pMXs-hSOX2, pMXs-hKLF4, pMXs-hc-MYC (Addgene) [16]. Fibroblasts expressing the mouse *Slc7a1* gene were then infected with retroviral cocktail. Next day, the medium was replaced with DMEM supplemented with 10% FBS (wt/vol.). After 6 days of transduction, infected fibroblasts were re-seeded on mouse fibroblast STO cell line feeder cells [17]. The medium was replaced the following day with human ES cell medium (ReproCELL; ReproCELL, Yokohama, Japan) supplemented with 4 ng/ml basic fibroblast growth factor (Wako, Osaka, Japan) and changed every 2 days. Starting 4 weeks after infection, colonies were picked on the basis of their morphological resemblance to human ES cell colonies and transferred on to mouse fibroblast STO cell line feeder cells in six-well plates; we defined this stage as passage one. Cultures were maintained on mouse fibroblast STO cell line feeders and passaged every 5 to 7 days enzymatically using 0.25% (wt/vol.) trypsin with 0.1 mg/ml collagenase type IV. Two human ES cell lines (H9 and KhES-1) and two human iPS cell lines (B7 and G1) were cultured and collected for genomic DNA analysis [4, 18–20].

Quantitative assessment of mtDNA mutation frequencies by Invader assay The primary probes and the invader oligo used to detect A3243G heteroplasmy were as follows: primary probe for 3243A: 5′-CGCGCCGAGGAGCCCGG TAATCGC<amino>–3′; primary probe for 3243G: 5′-ACG GACGCGGAGGGCCCGGTAATCG<amino>–3′; common Invader oligo: 5′-CCCACCCAAGAACAGGGTTTGTTAA GATGGCAGT-3′. The first 10 and 12 positions in the primary

probes represent the 5′ flap of Invader reaction. The cleavage enzyme, fluorescence resonance energy transfer probe, signal probe and Invader oligo were added to the microplates, including diluted plasmids that included the primary probe/Invader oligo binding region, after which the Invader assay was carried out as previously described [21]. The plates were incubated at 63°C in the fluorescence microplate reader (FluoDia-T70; Otsuka Electronics, Osaka, Japan). Fluorescence values for carboxyfluorescein (3243A; wavelength/bandwidth: excitation 485/20 nm; emission 530/25 nm) and Redmond red (3243G; excitation 560/20 nm; emission 620/40 nm) were measured every 2 min for a period of 4 h. To detect A3243G heteroplasmy, we calculated the copy number of 3243A and 3243G with a standard curve using quantitative Invader assay as described [21, 22]. The A3243G ratio was based on the ratio of the all-copy (3243A and 3243G) to the 3243A copy. In this assay, the lowest detection limit of the mutation frequency is 2%. The mtDNA A3243G mutation was also analysed by PCR-RFLP or fluorescent correlation spectroscopy [23–25].

Immunocytochemistry and alkaline phosphatase staining Immunocytochemistry was carried out as previously described [26]. The anti-human primary antibodies included: stage-specific embryonic antigen (SSEA)-1, SSEA-3, SSEA-4, tumour rejection antigen (TRA)-1-60, TRA-1-81 (all from Stemgent, San Diego, CA, USA), Nanog homeobox (NANOG) (R&D Systems, Minneapolis, MN, USA), β3 tubulin (Millipore, Temecula, CA, USA), α-smooth muscle actin (α-SMA) (Sigma-Aldrich, Saint Louis, MO, USA), forkhead box A2 (FOXA2) (Cell Signaling Technology, Danvers, MA, USA) and SRY (sex determining region Y)-box (SOX)17 (R&D Systems).

For immunofluorescence, Alexa Fluor 488 goat anti-mouse IgM, Alexa Fluor 488 goat anti-rat IgM, Alexa Fluor 488 goat anti-mouse IgG, Alexa Fluor 546 rabbit anti-goat IgG and Alexa Fluor 546 goat anti-mouse IgG (all from Molecular Probes, Eugene, OR, USA) served as the secondary antibody. Alkaline phosphatase activity was detected using a kit (Alkaline Phosphatase Staining Kit; Stemgent). Images were captured using a microscope (Olympus IX81; Olympus, Tokyo, Japan).

Karyotype analysis Standard G-banding chromosome analysis was performed in the Nihon Gene Research Laboratories (Sendai, Japan) or Chromosome Science Lab (Sapporo, Japan). Selected iPS clones (mitochondrial disease-specific [Mt-iPS] patient 1 [Mt1] clone 1 [Mt1-1], Mt1-4, Mt-iPS patient 2 [Mt2] clone 3 [Mt2-3] and Mt2-6) were analysed at passages 18 to 27.

Bisulphite genomic sequencing Genomic DNA (1 μg) from Mt-iPS cells was processed for bisulphite modification using a kit (EZ DNA Methylation Gold; Zymoresearch, Irvine, CA, USA). The cytosine guanine dinucleotide-rich promoter regions of *OCT4* (also known as *POU5F1*) and *NANOG* were selected to be amplified by PCR with ExTaq Hot start (Takara, Kyoto, Japan). The PCR products were subcloned into pCR4 vector (Life Technologies, Carlsbad, CA, USA). Ten clones of each sample were verified by sequencing with Sp6 universal primer.

Short tandem repeat analysis The genomic DNA was used for PCR with Cell ID System (Promega, Madison, WI, USA) and analysed by genetic analyser (ABI PRISM 3100) and GeneMapper version 3.5 (both from Applied Biosystems, Foster City, CA, USA).

In vitro differentiation by embryoid body formation and M15 co-culture Spontaneous differentiation through embryoid body (EB) formation was initiated by dissociation of Mt-iPS cells using collagenase/trypsin treatment, with subsequent transfer to low-attachment multi-well plates in ReproCELL medium. The medium was changed every second day. After 8 days of floating culture, tentative iPS (Mt-iPS) clones formed EBs and were transferred to 0.1% (wt/vol.) gelatin-coated plates to induce further differentiation for 8 days. Differentiated markers such as β3-tubulin, α-SMA and FOXA2 were analysed by immunocytochemistry.

Endodermal differentiation was performed according to Shiraki et al. [27]. In brief, dissociated Mt-iPS cells were inoculated on to multi-well plates containing a feeder layer of mitomycin C-treated M15 cells [28] in medium (DMEM supplemented with 10% FBS (wt/vol.) and penicillin/streptomycin; Invitrogen). The medium was changed every second day. After 2 weeks of culture, genomic DNA was extracted for the Invader assay. Endodermal differentiation was confirmed by immunocytochemistry with antibodies against FOXA2 and SOX17.

Teratoma formation Approximately 5×10^5 iPS cells were collected by collagenase/trypsin treatment and injected into the testicles of 7- to 12-week-old severe combined immunodeficient (SCID) mice. Teratomas were collected 9 to 12 weeks after injection and fixed with 10% (wt/vol.) buffered neutral formalin. Paraffin-embedded tissues were sectioned and stained with haematoxylin and eosin. Animal studies were conducted in accordance with our institutional guidelines and approved by Kyoto University Animal Care Committee.

Determination of mtDNA content Genomic DNA was extracted from blood, fibroblasts and Mt-iPS cells using a kit (DNeasy Tissue Kit; Qiagen, Valencia, CA, USA) or a standard established protocol [29]. The extracted DNA samples were stored at 4°C until assay. The relative mtDNA

copy numbers were measured by real-time PCR and corrected by measurement of the nuclear DNA [30]. The primers for mitochondrial *ND5* gene were 5′-AGGCGCTATCAC CACTCTGTTCG-3′ and 5′-AACCTGTGAGGAAAGG TATTCCTG-3′. The primers for nuclear *CF* (also known as *CFTR*) gene were 5′-AGCAGAGTACCTGAAACAGGAA-3′ and 5′-AGCTTACCCATAGAGGAAACATAA-3′. The PCR was performed using StepOnePlus Real-Time PCR (Applied Biosystems) and a quantitative PCR mix kit (Thunderbird SYBR qPCR Mix; Toyobo, Osaka, Japan). DNA (80 ng) was mixed with 10 μl SYBR qPCR containing 6 pmol of forward and reverse primers, and with ROX reference dye in a final volume of 20 μl. The PCR conditions were 1 min at 95°C, followed by 40 cycles of denaturation at 95°C for 15 s and of annealing and primer extension at 60°C for 60 s. Standard curves were generated using serial dilutions of plasmid DNA containing the PCR amplicons cloned into pGEM-T Easy (Promega). The threshold cycle number values of *ND5* and *CF* were determined in two DNA duplicate samples. The amplified products were denatured and re-annealed at different temperature points to detect their specific melting temperature.

Sample mtDNA content (mtDNA copies per cell) were calculated using the formula (*ND5* gene copies/*CF* gene copies)×2=mtDNA copies per cell.

Results

Generation of iPS cells from diabetic patients with the mtDNA A3243G mutation Skin biopsies were obtained from two Japanese patients who had diabetes mellitus, came from different families and carried the mtDNA A3243G mutation. Patient 1 (Mt1) was a 38-year-old man and patient 2 (Mt2) was a 46-year-old woman. Their clinical data are given in Table 1. Mt1 presented at 31 years of age with thirst, polydipsia, polyuria, tiredness and loss of body weight. His blood glucose concentration was 38.4 mmol/l and his HbA_{1c} level was 14.3% (132 mmol/mol). He responded well to insulin therapy as a way to control his diabetes. Mt2 was diagnosed with gestational diabetes at 24 years of age. She had a progressive hearing impairment. She had also suffered from epilepsy since the age of 27 years and had been treated with valproic acid. At 31 years of age she developed diabetic ketoacidosis and began insulin therapy. Both patients had a positive family history of maternal diabetes mellitus. The A3243G mtDNA mutation was identified by sequencing of PCR products amplified from peripheral blood genomic DNA from both patients (data not shown).

Two fibroblast lines (Mt1-fibro and Mt2-fibro) were obtained from skin biopsies of the two patients. Each fibroblast line was cultured and infected with a combination of retroviruses encoding the transcription factors octamer-binding protein 4 (OCT4), SOX2, proto-oncogene c-Myc (c-MYC) and Kruppel-like factor 4 (KLF4) [4]. Starting 4 weeks after infection, colonies were selected on the basis of their morphological resemblance to human ES cell colonies and expanded. We were able to isolate four (Mt1-1 to -4) and 10 (Mt2-1 to -10) putative iPS (Mt-iPS) clones from Mt1-fibro and Mt2-fibro lines, respectively.

mtDNA mutation frequencies in Mt-iPS cells The presence and levels of heteroplasmy in the patient-derived blood cells, fibroblasts (Mt1-fibro and Mt2-fibro) and putative iPS clones (Mt1-1 to -4 and Mt2-1 to -10) were evaluated (Fig. 1a). The Invader assay was used to quantify the heteroplasmy of the mtDNA A3243G mutation in Mt-iPS cells [31–33]. This method was originally developed to genotype single nucleotide polymorphisms and has been used to genotype mtDNA mutations and to quantify heteroplasmy. It is one of the most accurate ways of determining mtDNA heteroplasmy [34]. The passage numbers at which Mt-iPS cells were collected for the Invader assay were: Mt1-1 passage 12; Mt1-2 passage 16; Mt1-3 passage 17; Mt1-4 passage 14; Mt2-1 passage 9; Mt2-2 passage 8; Mt2-3 passage 10; Mt2-4 passage 9; Mt2-5 passage 10; Mt2-6 passage 10; Mt2-7 passage 7; Mt2-8 passage 7; Mt2-9 passage 9; Mt2-10 passage 11. Mutation frequencies in the peripheral blood cells from both patients were 24% (Mt1-blood 24%, Mt2-blood 24%). Skin-derived fibroblasts from both patients showed similar levels of mutation frequency compared with those of blood cells from the same patients (Mt1-fibro 18%, Mt2-fibro 24%). However, two of four Mt1-iPS clones (Mt1-1 and Mt1-2) and six of 10 Mt2-iPS clones (Mt2-1, Mt2-2, Mt2-3, Mt2-4, Mt2-7, Mt2-8) showed undetectable levels (<2%) of the A3243G mutation. Furthermore, marked elevations of the mutation frequencies compared with those of the original fibroblast lines were detected in other iPS lines (Mt1-3 51%, Mt1-4 87%, Mt2-5 83%, Mt2-6 69%, Mt2-9 79%, Mt2-10 74%). No significant associations were found between culture passage number of Mt-iPS cells and the mutation frequency. The absence and presence of the mutation were confirmed by PCR-RFLP and by gene analysis by fluorescence correlation spectroscopy [24, 25].

The mutation frequency of the fibroblasts was further assessed (Fig. 1b). The fibroblasts from patient 2 (Mt2-fibro) were cultured until passage 16 (for over 2 months). Fibroblast cell cloning by limiting dilution was performed from parental Mt2-fibro at passage five, and five fibroblast clones were obtained (Mt2-fibro-clone). Genomic DNA was extracted from Mt2-fibro at various passage points and from the five Mt2-fibro-clones at about 4 weeks after the cloning procedure. The mutation frequencies in Mt2-fibro gradually increased with increasing passage number of the cells

Table 1 Information on patient donors for generation of Mt1-iPS and Mt2-iPS cell lines

Patient	Age (years)	Sex	Family history	mtDNA mutation	Clinical abnormalities	BMI (kg/m^2)	Medication	HbA_{1c} (%)	
								%	mmol/mol
Mt1	38	Male	Mother: diabetes mellitus, cardiomyopathy	A3243G	Diabetes mellitus	18	Insulin 33 U/day	8.2	66.1
Mt2	46	Female	Mother: diabetes mellitus	A3243G	Diabetes mellitus, sensorineural hearing loss, epilepsy, cardiomyopathy	22	Insulin 30 U/day, valproic acid 600 mg/day	7.0	53.0

(Fig. 1b). All the Mt2-fibro-clones displayed high mutation frequencies and no mutation-free fibroblast clones were observed (Fig. 1b).

Characterisation of the Mt-iPS cells generated All the Mt-iPS clones showed typical human ES cell-like morphology (Fig. 2a, ESM Fig. 1). Mt-iPS cells were positive for alkaline phosphatase activity, and the pluripotent stem cell markers SSEA-3, SSEA-4, TRA-1-60, TRA-1-81 and NANOG were detected by immunocytochemical analyses in all 14 clones (Fig. 2a, ESM Fig. 1) [35]. Mt-iPS cells did not produce SSEA-1 except for a few cells at the edge of the colonies (Fig. 2a, ESM Fig. 1). The morphological and immunocytochemical characteristics of mutation-free and mutation-rich Mt-iPS cells were indistinguishable.

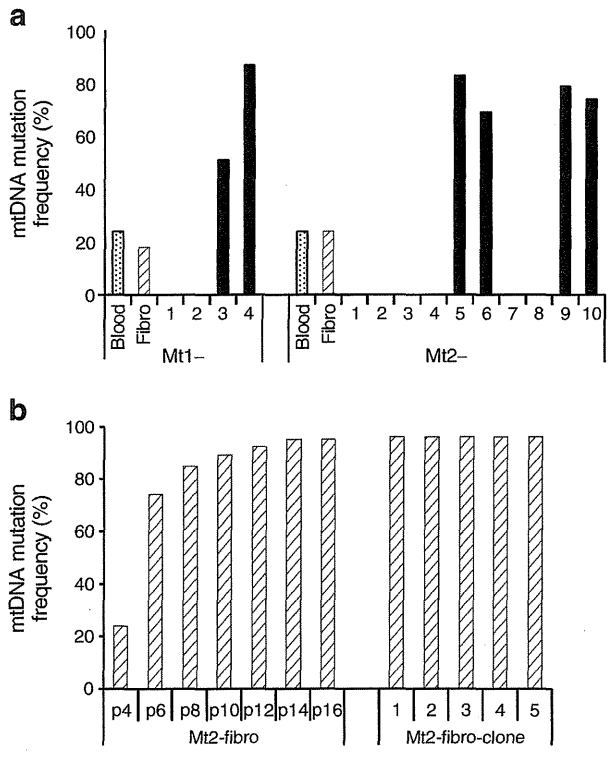

Fig. 1 mtDNA mutation frequencies in Mt-iPS cells. **a** mtDNA A3243G mutation frequencies in patient-derived blood cells (Mt1-blood, Mt2-blood), original fibroblasts (Mt1-fibro, Mt2-fibro) and Mt-iPS clones (Mt1-1 to Mt1-4, Mt2-1 to Mt2-10). Mt-iPS cells were collected at the following passage (p) numbers: Mt1-1 p12, Mt1-2 p16, Mt1-3 p17, Mt1-4 p14, Mt2-1 p9, Mt2-2 p8, Mt2-3 p10, Mt2-4 p9, Mt2-5 p10, Mt2-6 p10, Mt2-7 p7, Mt2-8 p7, Mt2-9 p9, Mt2-10 p11. **b** mtDNA A3243G mutation frequencies in Mt2-derived fibroblasts at various culture passage numbers and in isolated fibroblast clones. Limiting dilution was performed from the original fibroblasts (Mt2-fibro) at passage five and five fibroblast clones were obtained

To examine whether Mt-iPS clones are cytogenetically normal, karyotyping analyses were performed on selected Mt-iPS cells at passages 18 to 27. Both mutation-free (Mt1-1 and Mt2-3) and mutation-rich (Mt1-4 and Mt2-6) Mt-iPS clones from both patients maintained a normal karyotype (Fig. 2b, ESM Fig. 2).

Bisulphite genomic sequencing analyses evaluating the methylation statuses of cytosine guanine dinucleotides in the promoter regions of *OCT4* and *NANOG* revealed that they were highly unmethylated (Fig. 2c), indicating epigenetic reprogramming to pluripotency.

To confirm that the Mt-iPS clones were indeed derived from the patients, we performed DNA fingerprinting analyses with short tandem repeat markers. The short tandem repeat profiles of the Mt-iPS clones matched perfectly to those of their parental fibroblasts and of blood cells obtained from the patients (ESM Table 1). Thus, the Mt-iPS clones were indeed derived from the patients and were not a result of contamination.

Pluripotency of Mt-iPS cells by in vitro and in vivo differentiation Pluripotent cells are by definition capable of differentiating into cell types derived from each of the three embryonic germ layers [18]. To determine the differentiation ability of Mt-iPS cells in vitro, suspension culture for the formation of EBs was used [36]. After 8 days in suspension culture, iPS cells formed ball-shaped structures. These EBs were transferred to gelatin-coated plates and further cultured for another 8 days. Attached cells showed various types of morphologies, including those resembling neuronal cells, cobblestone-like cells and epithelial cells. Immunocytochemistry detected cells positive for β3-tubulin (a marker of ectoderm), α-SMA (a marker of mesoderm) or FOXA2 (a marker of endoderm) (Fig. 3a, ESM Fig. 3a). We

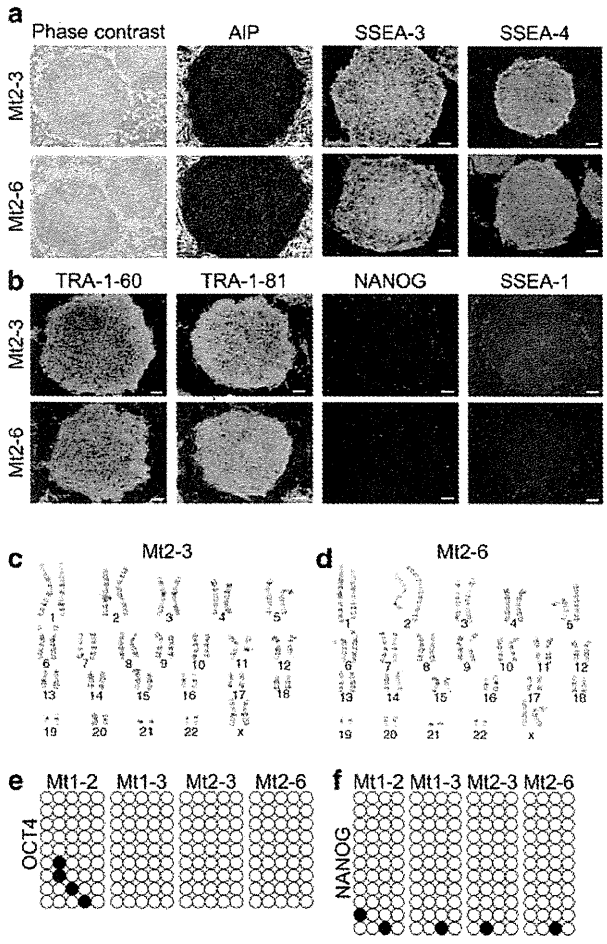

Fig. 2 Characterisation of generated Mt-iPS cells. **a, b** Colonies of Mt-iPS cells (Mt2-3 and Mt2-6) grown on mouse fibroblast STO cell line feeder cells showing human-ES-cell-like morphology. The detection of (**a**) alkaline phosphatase activity (AIP) and immunofluorescence analyses for the presence of the pluripotency markers SSEA-3, SSEA-4, and (**b**) TRA-1-60, TRA-1-81, NANOG and SSEA-1 are indicated. Scale bars 200 μm. **c** Karyotyping of Mt-iPS cells Mt2-3 and (**d**) Mt2-6 at passage 22. **e** Bisulphite genomic sequencing of the promoter regions of *OCT4* and (f) *NANOG*. White circles, unmethylated cytosine guanine dinucleotides; black circles, methylated cytosine guanine dinucleotides

found that all Mt-iPS clones were able to differentiate into three germ layers in vitro.

To determine pluripotency in vivo, we transplanted Mt-iPS cells into the testicles of SCID mice. At 9 weeks after injection, tumour formation was observed. Histological examination showed that the tumours contained various tissues, including pigmented epithelium (ectoderm), cartilage (mesoderm) and gut-like epithelial tissues (endoderm) (Fig. 3b, ESM Fig. 3b). Thus, Mt-iPS clones were able to spontaneously differentiate into derivatives of all three germ layers in vivo.

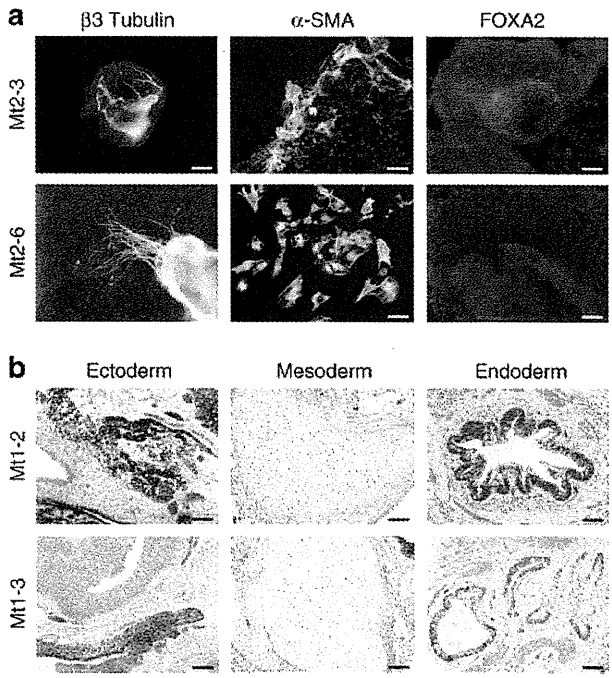

Fig. 3 Pluripotency of Mt-iPS cells by in vitro and in vivo differentiation. **a** In vitro differentiation of Mt-iPS cells (Mt2-3, Mt2-6) revealed their potential to generate cell derivatives of all three primary germ cell layers. Immunofluorescence analyses showed markers of neurectoderm (β3-tubulin), mesoderm (α-SMA) and endoderm (FOXA2). Images are overlays with a nuclear stain (DAPI). **b** Teratoma formation occurred after injection of Mt-iPS cells (Mt1-2, Mt1-3) into the testes of SCID mice (Japan Clea, Tokyo, Japan). Haematoxylin and eosin stainings of teratoma sections show derivatives of ectoderm (pigmented epithelial cells), mesoderm (cartilage) and endoderm (gut-like glandular structures). Scale bars, 100 μm

Influence of culture passage number and differentiation on mtDNA mutation frequencies in Mt-iPS cells We examined whether or not the mutation frequencies of Mt-iPS clones were fixed over the course of cell culturing and passage (Fig. 4a). Analysis of the same clones at various passage numbers revealed that no induction of mutation was observed in mutation-free Mt-iPS clones (Mt1-1, Mt1-2, Mt2-1, Mt2-3 and Mt2-8). Mutation frequencies of the mutation-rich Mt-iPS clones were relatively constant across passages (Mt1-3, Mt1-4, Mt2-6 and Mt2-10).

The influence of differentiation on mutation frequency was also examined in all the Mt-iPS clones (Fig. 4b). Analysis of the same clones in an undifferentiated state and after 16 days of differentiation as a result of spontaneous differentiation (EB formation) or directed differentiation into endodermal lineage (M15 co-culture) (ESM Fig. 4) showed no induction of mutation in mutation-free Mt-iPS clones (Mt1-1, Mt1-2, Mt2-1, Mt2-2, Mt2-3, Mt2-4, Mt2-7 and Mt2-8). The mutation frequencies of the mutation-rich Mt-iPS clones were relatively constant after differentiation (Mt1-3, Mt1-4, Mt2-5, Mt2-6, Mt2-9 and Mt2-10).

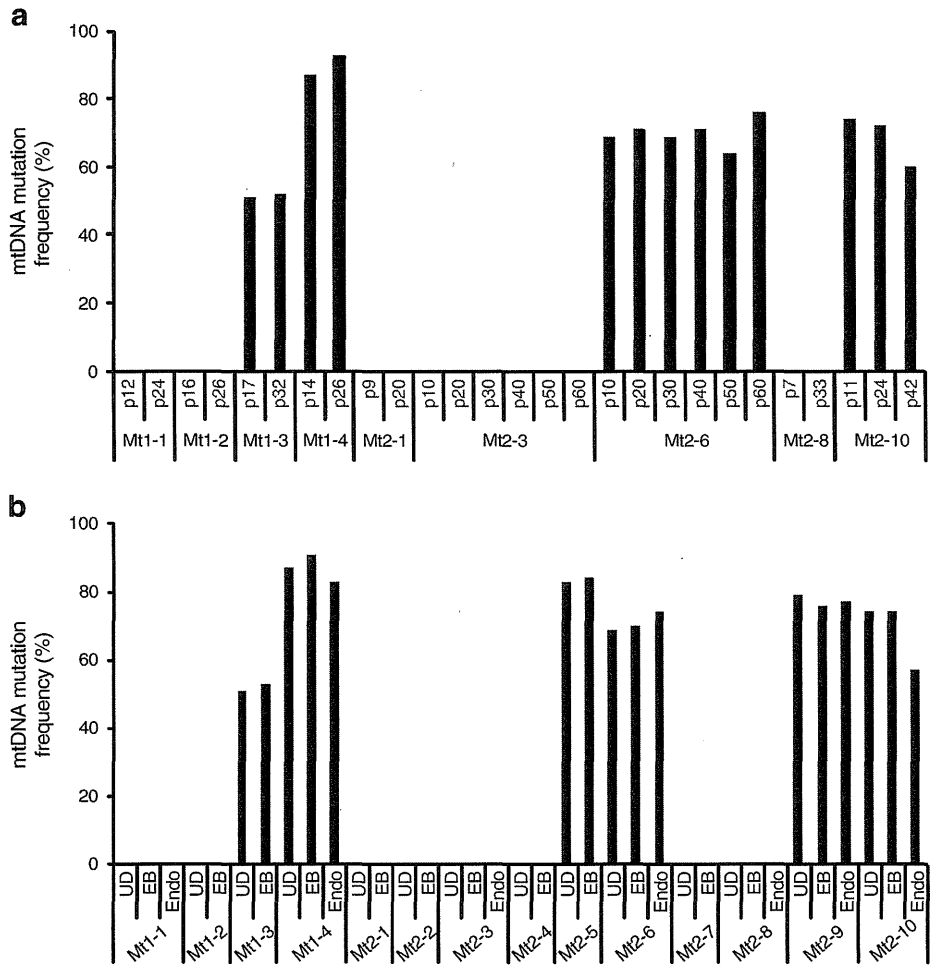

Fig. 4 Influence of culture passage number and differentiation on mtDNA mutation frequencies in Mt-iPS cells. **a** mtDNA A3243G mutation frequencies in undifferentiated Mt-iPS clones at various culture passage (p) numbers as indicated. **b** mtDNA A3243G mutation frequencies in undifferentiated (UD), differentiated EB (EB) and endodermal (Endo) states of Mt-iPS clones

mtDNA content in Mt-iPS cells The mtDNA content (mitochondrial genome copies per cell) in the blood cells, fibroblasts (Mt1-fibro and Mt2-fibro) and iPS clones was determined by quantitative genomic PCR (Fig. 5).

The skin fibroblast mtDNA content (Mt1-fibro 553 copies/cell; Mt2-fibro 4296 copies/cell) was higher than that in the peripheral blood (Mt1-blood 196 copies/cell; Mt2-blood 60 copies/cell). The mtDNA content of Mt-iPS cells at early passage was slightly lower than that in the original fibroblast cultures (Mt1-1 passage 12 454 copies/cell; Mt1-4 passage 14 151 copies/cell; Mt2-3 passage 10 2,100 copies/cell; Mt2-6 passage 10 1,709 copies/cell) (Fig. 5 and data not shown). The mtDNA content of Mt-iPS cells markedly decreased to levels close to those of human ES (H9 passage 87 79 copies/cell; KhES-1 passage 78 78 copies/cell) and iPS (B7 passsage 54 150 copies/cell; G1 passage 40 94 copies/cell) cells by passage number 20 (Mt1-4 passage 26 42 copies/cell; Mt2-3 passage 20 49 copies/cell; Mt2-6 passage 20 45 copies/cell) and was maintained thereafter (Mt2-3 passage 30 68 copies/cell; Mt2-6 passage 30 50 copies/cell). The mtDNA content of fibroblasts and iPS cells from Mt1 (Mt1-fibro, Mt1-1 passage 12 and Mt1-4passage 14) were lower than those from Mt2 (Mt2-fibro, Mt2-3

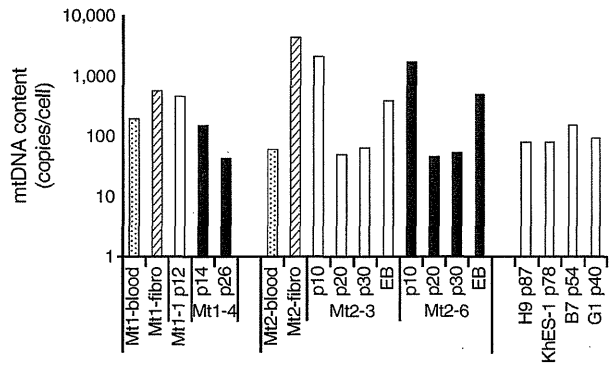

Fig. 5 mtDNA content in Mt-iPS cells. mtDNA content (copies/cell) in blood cells, fibroblasts, mutation-free iPS clones (Mt1-1, Mt2-3 white bars) and mutation-rich iPS clones (black bars). mtDNA from two human ES cell lines (H9 and KhES1) and two human iPS cell lines (B7 and G1) are also shown. p, passage. Mt-iPS cells at around p30 were used for EB formation and assayed for mtDNA contents (Mt2-3 EB, Mt2-6 EB)

passage 10 and Mt2-6 passage 10), although the content of each Mt-iPS clone was variable (data not shown).

The mtDNA copy number increased seven- to tenfold after EB differentiation (Mt2-3 passage 24-derived EB 384 copies/cell; Mt2-6 passage 24-derived EB 484 copies/cell). Major differences in mtDNA content were not found between mutation-free and mutation-rich iPS cells (Fig. 5 and data not shown).

Discussion

In the present study, we established human iPS cell lines from male and female diabetic patients with the mtDNA A3243G mutation. These cells have the features of pluripotent human ES cells, including the ability to differentiate into cell types of all embryonic lineages.

A striking feature of Mt-iPS shown in the present study is their bimodal levels of heteroplasmy. The mtDNA mutation frequencies decreased to undetectable levels in about half of the clones, while the other half showed a large increase in the levels of mutation heteroplasmy compared with those in the patients' original fibroblasts. The mechanisms underlying this phenomenon remain unclear; however, several possibilities exist in terms of the timing of heteroplasmy segregation. One is that the heteroplasmy levels in Mt-iPS clones simply reflect those in the original single fibroblast from which the iPS clones were derived. This is based on the assumption that the population of fibroblasts is bimodal (mutation-rich and mutation-free) with regard to levels of heteroplasmy, but we were not able to isolate any mutation-free fibroblast clone and hence could find no evidence of extreme mosaicism in the original fibroblasts. The second possibility is that changes in the levels of heteroplasmy occur during serial in vitro culture of Mt-iPS cells. Previous reports have shown age-related directional selection for different mtDNA genotypes in mouse tissues [37]; however, this is unlikely in our study because passage number did not significantly affect the mutation frequencies of Mt-iPS cells. The third and most likely possibility is that changes in the levels of heteroplasmy occur during reprogramming of patients' fibroblasts to iPS cells. Substantial shifts in the levels of mitochondrial heteroplasmy have been demonstrated to occur between single mammalian generations, and neutral mitochondrial genotypes have also been demonstrated to segregate in different directions in offspring from the same female (rapid segregation of mitochondrial genotype) [38–40]. Random partitioning of organelles with few mtDNA molecules into germ cells could account for the small number of segregating units and lead to the rapid segregation of polymorphic mtDNA species in the progeny.

The A3243G transition in the tRNA *Leu* gene is one of the most frequent mitochondrial mutations [2]. The phenotypic expression of the mutation is variable and may be associated with maternally inherited diabetes mellitus and deafness syndrome, myoclonic epilepsy and ragged-red fibres (MERRF) syndrome, MELAS/MERRF overlap syndrome, maternally inherited Leigh syndrome, and chronic external ophthalmoplegia or Kearns–Sayre syndrome. This heterogeneity is considered to result from the variable levels of heteroplasmy and the variability of tissue-specific thresholds for mitochondrial functions required for normal development and physiology [41]. There is currently no specific therapy or cure. The precise mechanisms for the generation of heteroplasmy and of mitochondrial dysfunction in these diseases remain to be elucidated. Mt-iPS cells offer several significant advantages for this research. The analysis of the process of iPS cell generation might help to clarify the mechanisms of mtDNA germ line segregation. This might further clarify the mode of inheritance of mitochondrial diseases, enabling prefertilisation diagnosis to be performed. We might also be able to study the process of mtDNA somatic segregation toward the target tissues involved in mitochondrial diseases after the induction of differentiation. Mutation-rich Mt-iPS cells should be useful as new types of disease models, in which the initiation and progression of the diseases can be studied. In this context, mutation-free Mt-iPS cells sharing the same nuclear genetic background could serve as ideal negative controls. These approaches could improve understanding of the cause of the disease and lead to the development of efficient preventive and therapeutic strategies. Ultimately, patient-specific and mutation-free Mt-iPS cells might be useful as a supplement or an alternative to disease-affected tissues in future. In this study, we generated Mt-iPS cells by retroviral transduction of *OCT4*, *SOX2*, *c-MYC* (also known as *MYC*) and *KLF4*; however, genomic integration of these transgenes increases the risk of tumorigenicity. By generating integration-free human iPS cells, we could safely transplant mtDNA-mutation-corrected cells without the use of potentially harmful DNA recombination technology [42]. mtDNA content is known to be a major determinant of mitochondrial gene expression [43]. Undifferentiated mouse and human ES cells have very low levels of mtDNA content (<100 copies/cell), but this rapidly increases up to several thousand-fold during differentiation [44–47]. However, it remains to be determined whether human iPS cells are able, like ES cells, to regulate their mtDNA copy number in their undifferentiated state. We have revealed here that the mtDNA content in Mt-iPS cells at early passage (around passage 10) is similar to that of the original fibroblasts, and that the mtDNA content at later passages (after passage 20) is similar to that of human ES cells. This indicates that the number of mitochondria gradually adapts to the new stem cell environment in iPS cells. Although compensatory amplification of the mitochondrial genome has been reported in patients with mtDNA mutations, the mtDNA content is relatively constant among Mt-iPS

clones, despite a wide variation in heteroplasmy levels [48–50]. These results also indicate that the cell viability and stemness are unaffected at the low metabolic demand of undifferentiated iPS cells, irrespective of the presence or absence of the A3243G mutation.

In conclusion, we have generated mitochondrial Mt-iPS cells. About half of the clones had undetectable levels of the mutation. By overcoming the immunological and ethical problems associated with ES cells, these Mt-iPS cells could provide a powerful new tool with which to investigate organ involvement and pathogenic mechanisms, and also to screen for new drugs in specific diseases, as well as opening new avenues for autologous cell transplantation therapy.

Acknowledgements We thank K. Nakada and K. Kuwahara for helpful discussions.

Funding This work was supported in part by research grants from: the Leading Project of the Ministry of Education, Culture, Sports, Science and Technology of Japan; the Ministry of Health, Labour and Welfare of Japan; the Takeda Medical Research Foundation; the Smoking Research Foundation; Suzuken Memorial Foundation; Japan Foundation of Applied Enzymology; Novo Nordisk (Insulin Research Award); and Lilly Education and Research Grant Office.

Contribution statement JF, Kazuhiro Nakao, MS, KH and Kazuwa Nakao contributed to study concept and design. JF, Kazuhiro Nakao, MN, EM, MN, DT, MH-S, IK, AW, IA and Kazuwa Nakao contributed to analysis and interpretation of data. JF, Kazuhiro Nakao, MS, MN, EM, MN, DT, MH-S, IK, AW, IA, KH and Kazuwa Nakao contributed to drafting of the manuscript. JF, Kazuhiro Nakao and Kazuwa Nakao contributed to critical revision of the manuscript for intellectual content. All the authors gave approval of the final version to be published.

Duality of interest The authors declare that there is no duality of interest associated with this manuscript.

References

1. May-Panloup P, Chretien MF, Malthiery Y, Reynier P (2007) Mitochondrial DNA in the oocyte and the developing embryo. Curr Top Dev Biol 77:51–83
2. Finsterer J (2009) Manifestations of the mitochondrial A3243G mutation. Int J Cardiol 137:60–62
3. Shoubridge EA, Wai T (2007) Mitochondrial DNA and the mammalian oocyte. Curr Top Dev Biol 77:87–111
4. Takahashi K, Tanabe K, Ohnuki M et al (2007) Induction of pluripotent stem cells from adult human fibroblasts by defined factors. Cell 131:861–872
5. Sone M, Itoh H, Yamahara K et al (2007) Pathway for differentiation of human embryonic stem cells to vascular cell components and their potential for vascular regeneration. Arterioscler Thromb Vasc Biol 27:2127–2134
6. Taura D, Noguchi M, Sone M et al (2009) Adipogenic differentiation of human induced pluripotent stem cells: comparison with that of human embryonic stem cells. FEBS Lett 583:1029–1033
7. Dimos JT, Rodolfa KT, Niakan KK et al (2008) Induced pluripotent stem cells generated from patients with ALS can be differentiated into motor neurons. Science 321:1218–1221
8. Ebert AD, Yu J, Rose FF Jr et al (2009) Induced pluripotent stem cells from a spinal muscular atrophy patient. Nature 457:277–280
9. Park IH, Arora N, Huo H et al (2008) Disease-specific induced pluripotent stem cells. Cell 134:877–886
10. Soldner F, Hockemeyer D, Beard C et al (2009) Parkinson's disease patient-derived induced pluripotent stem cells free of viral reprogramming factors. Cell 136:964–977
11. Liu J, Verma PJ, Evans-Galea MV et al (2011) Generation of induced pluripotent stem cell lines from Friedreich Ataxia patients. Stem Cell Rev 7:703–713
12. Carvajal-Vergara X, Sevilla A, D'Souza SL et al (2010) Patient-specific induced pluripotent stem-cell-derived models of LEOPARD syndrome. Nature 465:808–812
13. Raya A, Rodriguez-Piza I, Guenechea G et al (2009) Disease-corrected haematopoietic progenitors from Fanconi anaemia induced pluripotent stem cells. Nature 460:53–59
14. Maehr R, Chen S, Snitow M et al (2009) Generation of pluripotent stem cells from patients with type 1 diabetes. Proc Natl Acad Sci U S A 106:15768–15773
15. Ohnuki M, Takahashi K, Yamanaka S (2009) Generation and characterization of human induced pluripotent stem cells. Curr Protoc Stem Cell Biol Chapter 4: Unit 4A 2
16. Morita S, Kojima T, Kitamura T (2000) Plat-E: an efficient and stable system for transient packaging of retroviruses. Gene Ther 7:1063–1066
17. McMahon AP, Bradley A (1990) The Wnt-1 (int-1) proto-oncogene is required for development of a large region of the mouse brain. Cell 62:1073–1085
18. Thomson JA, Itskovitz-Eldor J, Shapiro SS et al (1998) Embryonic stem cell lines derived from human blastocysts. Science 282:1145–1147
19. Fujioka T, Yasuchika K, Nakamura Y, Nakatsuji N, Suemori H (2004) A simple and efficient cryopreservation method for primate embryonic stem cells. Int J Dev Biol 48:1149–1154
20. Nakagawa M, Koyanagi M, Tanabe K et al (2008) Generation of induced pluripotent stem cells without Myc from mouse and human fibroblasts. Nat Biotechnol 26:101–106
21. Yamamoto M, Kakihana K, Ohashi K et al (2009) Serial monitoring of T315I BCR-ABL mutation by Invader assay combined with RT-PCR. Int J Hematol 89:482–488
22. Hall JG, Eis PS, Law SM et al (2000) Sensitive detection of DNA polymorphisms by the serial invasive signal amplification reaction. Proc Natl Acad Sci U S A 97:8272–8277
23. Kadowaki T, Kadowaki H, Mori Y et al (1994) A subtype of diabetes mellitus associated with a mutation of mitochondrial DNA. N Engl J Med 330:962–968
24. Katagiri H, Asano T, Ishihara H et al (1994) Mitochondrial diabetes mellitus: prevalence and clinical characterization of diabetes due to mitochondrial tRNA(Leu(UUR)) gene mutation in Japanese patients. Diabetologia 37:504–510
25. Palo K, Mets U, Jager S, Kask P, Gall K (2000) Fluorescence intensity multiple distributions analysis: concurrent determination of diffusion times and molecular brightness. Biophys J 79:2858–2866
26. Nagano M, Katagiri S, Takahashi Y (2006) ATP content and maturational/developmental ability of bovine oocytes with various cytoplasmic morphologies. Zygote 14:299–304
27. Shiraki N, Yoshida T, Araki K et al (2008) Guided differentiation of embryonic stem cells into Pdx1-expressing regional-specific definitive endoderm. Stem Cells 26:874–885
28. Larsson SH, Charlieu JP, Miyagawa K et al (1995) Subnuclear localization of WT1 in splicing or transcription factor domains is regulated by alternative splicing. Cell 81:391–401

29. Laird PW, Zijderveld A, Linders K, Rudnicki MA, Jaenisch R, Berns A (1991) Simplified mammalian DNA isolation procedure. Nucleic Acids Res 19:4293
30. Prigione A, Fauler B, Lurz R, Lehrach H, Adjaye J (2010) The senescence-related mitochondrial/oxidative stress pathway is repressed in human induced pluripotent stem cells. Stem Cells 28:721–733
31. Lyamichev V, Mast AL, Hall JG et al (1999) Polymorphism identification and quantitative detection of genomic DNA by invasive cleavage of oligonucleotide probes. Nat Biotechnol 17:292–296
32. Mashima Y, Nagano M, Funayama T et al (2004) Rapid quantification of the heteroplasmy of mutant mitochondrial DNAs in Leber's hereditary optic neuropathy using the Invader technology. Clin Biochem 37:268–276
33. Inagaki Y, Mashima Y, Fuse N, Ohtake Y, Fujimaki T, Fukuchi T (2006) Mitochondrial DNA mutations with Leber's hereditary optic neuropathy in Japanese patients with open-angle glaucoma. Jpn J Ophthalmol 50:128–134
34. Mazunin IO, Volodko NV, Starikovskaya EB, Sukernik RI (2010) Mitochondrial genome and human mitochondrial diseases. Mol Biol 44:665–681
35. Adewumi O, Aflatoonian B, Ahrlund-Richter L et al (2007) Characterization of human embryonic stem cell lines by the International Stem Cell Initiative. Nat Biotechnol 25:803–816
36. Itskovitz-Eldor J, Schuldiner M, Karsenti D et al (2000) Differentiation of human embryonic stem cells into embryoid bodies compromising the three embryonic germ layers. Mol Med 6:88–95
37. Jenuth JP, Peterson AC, Shoubridge EA (1997) Tissue-specific selection for different mtDNA genotypes in heteroplasmic mice. Nat Genet 16:93–95
38. Ashley MV, Laipis PJ, Hauswirth WW (1989) Rapid segregation of heteroplasmic bovine mitochondria. Nucleic Acids Res 17:7325–7331
39. Laipis PJ, van de Walle MJ, Hauswirth WW (1988) Unequal partitioning of bovine mitochondrial genotypes among siblings. Proc Natl Acad Sci U S A 85:8107–8110
40. Larsson NG, Tulinius MH, Holme E et al (1992) Segregation and manifestations of the mtDNA tRNA(Lys) A–>G(8344) mutation of myoclonus epilepsy and ragged-red fibers (MERRF) syndrome. Am J Hum Genet 51:1201–1212
41. Leonard JV, Schapira AH (2000) Mitochondrial respiratory chain disorders II: neurodegenerative disorders and nuclear gene defects. Lancet 355:389–394
42. Chou BK, Mali P, Huang X et al (2011) Efficient human iPS cell derivation by a non-integrating plasmid from blood cells with unique epigenetic and gene expression signatures. Cell Res 21:518–529
43. Williams RS, Salmons S, Newsholme EA, Kaufman RE, Mellor J (1986) Regulation of nuclear and mitochondrial gene expression by contractile activity in skeletal muscle. J Biol Chem 261:376–380
44. Cho YM, Kwon S, Pak YK et al (2006) Dynamic changes in mitochondrial biogenesis and antioxidant enzymes during the spontaneous differentiation of human embryonic stem cells. Biochem Biophys Res Commun 348:1472–1478
45. Facucho-Oliveira JM, Alderson J, Spikings EC, Egginton S, St John JC (2007) Mitochondrial DNA replication during differentiation of murine embryonic stem cells. J Cell Sci 120:4025–4034
46. Harvey A, Gibson T, Lonergan T, Brenner C (2010) Dynamic regulation of mitochondrial function in preimplantation embryos and embryonic stem cells. Mitochondrion 11:829–838
47. St John JC, Facucho-Oliveira J, Jiang Y, Kelly R, Salah R (2010) Mitochondrial DNA transmission, replication and inheritance: a journey from the gamete through the embryo and into offspring and embryonic stem cells. Hum Reprod Update 16:488–509
48. Wong LJ, Perng CL, Hsu CH et al (2003) Compensatory amplification of mtDNA in a patient with a novel deletion/duplication and high mutant load. J Med Genet 40:e125
49. Kim K, Lecordier A, Bowman LH (1995) Both nuclear and mitochondrial cytochrome c oxidase mRNA levels increase dramatically during mouse postnatal development. Biochem J 306:353–358
50. Ostronoff LK, Izquierdo JM, Enriquez JA, Montoya J, Cuezva JM (1996) Transient activation of mitochondrial translation regulates the expression of the mitochondrial genome during mammalian mitochondrial differentiation. Biochem J 316:183–191

One Dose of Ghrelin Prevents the Acute and Sustained Increase in Cardiac Sympathetic Tone after Myocardial Infarction

Daryl O. Schwenke, Takeshi Tokudome, Ichiro Kishimoto, Takeshi Horio, Patricia A. Cragg, Mikiyasu Shirai, and Kenji Kangawa

Department of Physiology (D.O.S., P.A.C.), University of Otago, Dunedin 9001, New Zealand; Departments of Biochemistry (T.T., I.K., T.H., K.K.) and Cardiac Physiology (M.S.), National Cerebral and Cardiovascular Center Research Institute, Osaka 565-8565, Japan

Acute myocardial infarction (MI) increases sympathetic nerve activity (SNA) to the heart, which exacerbates chronic cardiac deterioration. The hormone ghrelin, if administered soon after an MI, prevents the increase in cardiac SNA and improves early survival prognosis. Whether these early beneficial effects of ghrelin also impact on cardiac function in chronic heart failure has not yet been addressed and thus was the aim of this study. MI was induced in Sprague Dawley rats by ligating the left coronary artery. One bolus of saline (n = 7) or ghrelin (150 μg/kg, sc, n = 9) was administered within 30 min of MI. Two weeks after the infarct (or sham; n = 7), rats were anesthetized and cardiac function was evaluated using a Millar pressure-volume conductance catheter. Cardiac SNA was measured using whole-nerve electrophysiological techniques. Untreated-MI rats had a high mortality rate (50%), evidence of severe cardiac dysfunction (ejection fraction 28%; $P < 0.001$), and SNA was significantly elevated (102% increase; $P = 0.03$). In comparison, rats that received a single dose of ghrelin after the MI tended to have a lower mortality rate (25%; P = NS) and no increase in SNA, and cardiac dysfunction was attenuated (ejection fraction of 43%; $P = 0.014$). This study implicates ghrelin as a potential clinical treatment for acute MI but also highlights the importance of therapeutic intervention in the early stages after acute MI. Moreover, these results uncover an intricate causal relationship between early and chronic changes in the neural control of cardiac function in heart failure. **(*Endocrinology* 153: 2436–2443, 2012)**

Myocardial infarction (MI) is the most common cause of death in industrialized societies. This high morbidity has been strongly associated with an adverse and sustained increase in cardiac sympathetic nerve activity (SNA), which begins within the first hour of the initial infarction (1). Even for those who survive the immediate infarct, the sustained increase in cardiac SNA exacerbates the ischemic damage to cardiac tissue, stimulates ventricular modeling (2), reduces β-adrenergic receptor density (3) and signaling (4), and thus critically impairs the functional capacity of the heart.

Ever since its discovery in 1999 (5), the peptide hormone ghrelin (28 amino acids), which is released from the stomach wall, has been implicated in a diverse range of physiological functions. Originally identified as an endogenous ligand for the GH secretagogue receptor (GHS-R), ghrelin produces anabolic effects through the release of GH but also has pivotal roles in orexigenic regulation, glucose and lipid metabolism, neurohormonal control, energy and metabolic homeostasis, and cardiovascular function (see recent review in Ref. 6).

Importantly, ghrelin has been shown to improve cardiac function in patients suffering from end-stage chronic heart failure (7). Although the therapeutic effects of ghrelin have largely been attributed to the release of GH (7, 8), evidence is accumulating that supports a direct cardiopro-

ISSN Print 0013-7227 ISSN Online 1945-7170
Printed in U.S.A.

doi: 10.1210/en.2011-2057 Received December 3, 2011. Accepted February 23, 2012.
First Published Online March 20, 2012

Abbreviations: ABP, Arterial blood pressure; ANP, atrial natriuretic peptide; BNP, B-type natriuretic peptide; CO, cardiac output; CSNA, cardiac SNA; dp/dt_{max}, maximum rate of ventricular contraction; GAPDH, glyceraldehyde 3-phosphate dehydrogenase; GHS-R, GH secretagogue receptor; HR, heart rate; LAD, left anterior descending; LVEDV, left ventricular end-diastolic volume; LVP, left ventricular pressure; LVV, left ventricular volume; MI, myocardial infarction; P-V, pressure/volume; SNA, sympathetic nerve activity; SV, stroke volume.

tective effect of ghrelin through the central modulation of sympathetic nerve activity (9–11).

To date, there is a paucity of studies describing the treatment of myocardial ischemia within the first few hours of onset. Yet it is this time period when autonomic modulation of cardiac function becomes enhanced, in which the opportunity to improve outcome by therapeutic intervention is so great (1). We recently demonstrated using an anesthetized rat preparation that ghrelin, when given immediately following an acute MI, was able to prevent the increase in cardiac SNA and improve survival rate, at least for the length of the short-term protocol (~6 h) (12). Moreover, ghrelin was able to completely reverse the increase in cardiac SNA if administered within 2 h of the MI. Yet the clinical and scientific impact of these observations are negated if we do not further establish whether these early beneficial effects of ghrelin extend to long-term benefits, such as sustaining the reduced sympathetic tone and thus improving long-term outcome.

Therefore, in this study we aimed to determine whether the chronic adverse changes in cardiac SNA and function would be influenced by the early treatment of ghrelin after an acute MI.

Materials and Methods

Animals

All experiments were approved and conducted in accordance with the guidelines stipulated by the Animal Ethics Committee of the University of Otago, New Zealand (Permit 04/07). The guidelines conform to the Guide for the Care and Use of Laboratory Animals published by the United States National Institutes of Health. Experiments were conducted on 33 male Sprague Dawley rats (8 wk old; body weight ~ 280–340 g). All rats were on a 12-h light, 12-h dark cycle at 25 ± 1 C and provided with food and water *ad libitum*.

Surgical induction of myocardial infarction

Surgical procedures were performed using standard aseptic techniques. Rats were anesthetized with ketamine/dormitor (75/0.5 mg/kg, ip). Adequate anesthesia was confirmed by elimination of the limb withdrawal reflex. All animals received an injection of Caprofen analgesia (5 mg/kg, sc) and Strepcin antibiotics (0.1 ml/kg, sc) before surgery. Throughout the surgery body temperature was maintained at 37 C using a rectal thermistor coupled with a thermostatically controlled heating pad. The trachea was intubated and the lungs ventilated with a rodent ventilator (SN-480-7; Shinano, Tokyo, Japan). A left thoracotomy was performed between the second and third ribs, and a 7.0 Prolene suture was placed around the left anterior descending (LAD) coronary artery, which was located between the appendage of the left atrium and the base of the pulmonary artery and then subsequently removed (sham) or tightened (MI). Those rats that received an acute MI were treated with either saline (0.3 ml = MI+Saline) or one bolus dose of ghrelin (150 μg/kg, sc = MI+Ghr) within 30 min of the infarct procedure. The dose of ghrelin used in this study was based on its therapeutic efficiency in our prior study (12). Subsequently the thoracotomy and skin incisions were closed with sutures. Ghrelin was obtained from the Peptide Institute Inc.

Immediately after surgery, all animals received supplementary fluids (10 ml of warm saline, sc) and remained on the heating blanket during recovery from anesthesia. Rats were returned to their standard housing conditions in which they remained for 14 d before experimental data were collected. During this period the welfare of the rat was monitored by recording body weight, food and water consumption, observing general appearance and behavior, and cleaning and dressing wounds if required.

Arterial blood pressure and cardiac function measurements

Fourteen days after the initial MI, rats were anesthetized (urethane, 1.5 g/kg, ip), intubated and mechanically ventilated. The femoral artery and vein were cannulated for measurement of systemic arterial blood pressure (ABP) and fluid administration (saline at 3 ml/h), respectively. The right carotid artery was also cannulated with a 1.5 F Millar pressure/volume (P-V) catheter (model SPR-869), which was then advanced into the left ventricle for the continuous measurement of left ventricular pressure (LVP) and left ventricular volume (LVV). From these measurements, we were able to determine the left ventricular end-diastolic pressure and left ventricular end-diastolic volume (LVEDV), end-systolic pressure and volume, and calculate stroke volume (SV) and thus the cardiac output (CO). The Millar P-V catheter was calibrated using a sphygmomanometer (pressure), and volumetric cuvettes (volume) and hypertonic saline injections (for volumetric corrections), as previously described in detail (13).

Recording cardiac SNA

The stellate ganglion was exposed through a left thoracotomy between the first and second rib. The cardiac sympathetic nerve was identified as a branch from the stellate ganglion, dissected free of surrounding connective tissue and sectioned, and the proximal section (containing efferent fibers) was placed on a pair of platinum recording electrodes. The signal was filtered (low cutoff 0.1 kHz; high cutoff 1 kHz) and amplified and subsequently passed through an amplitude discriminator (model WD-2; Dagan Corp., Minneapolis, MN) for counting nerve discharge frequency (impulse frequency).

Data analysis

Raw SNA, impulse frequency, LVP, LVV, and ABP were continuously sampled at 4 KHz, 200 Hz, 400 Hz, 400 Hz, and 400 Hz, respectively, using a PowerLab data-acquisition system (model 8/S; AD Instruments Ltd., Dunedin, New Zealand). Heart rate (HR) was derived from the arterial systolic peaks. The maximum rate of ventricular contraction (dp/dt_{max}) and relaxation were derived from the LVP signal using the inherent analytical tools of the Powerlab system. The raw nerve signal was rectified and integrated (1 sec resetting interval) online, and the integrated nerve signal was displayed in real time.